

# RBF modeling of Incipient Motion of Plane Sand Bed Channels

Gopu Sreenivasulu, Bimlesh Kumar, and Achanta Ramakrishna Rao

**Abstract**—To define or predict incipient motion in an alluvial channel, most of the investigators use a standard or modified form of Shields' diagram. Shields' diagram does give a process to determine the incipient motion parameters but an iterative one. To design properly (without iteration), one should have another equation for resistance. Absence of a universal resistance equation also magnifies the difficulties in defining the model. Neural network technique, which is particularly useful in modeling a complex processes, is presented as a tool complimentary to modeling incipient motion. Present work develops a neural network model employing the RBF network to predict the average velocity  $u$  and water depth  $y$  based on the experimental data on incipient condition. Based on the model, design curves have been presented for the field application.

**Keywords**—Incipient motion, Prediction error, Radial-Basis function, Sediment transport, Shields' diagram.

## I. INTRODUCTION

INCIPIENT motion in plane bed sand channels is described as the force required to initiate motion. At the point of incipient motion, a particle experiences a critical shear stress that sets it in motion. If the force of the flowing water is less than the critical shear stress, particles will remain motionless. Only when the force exerted by the flowing water is greater than or equal to the critical shear stress movement will be observed. Incipient motion has been studied extensively over the past years following the work by Shields [1], who presented a semi-empirical approach to incipient motion. Much of the subsequent research into incipient motion builds on the original work of Shields. The factors that are important in the determination of incipient motion are the shear stress  $\tau$ , the difference in density between sediment and fluid  $\rho_s - \rho$ , diameter of the particle  $d$ , the kinematic viscosity  $\nu$  and the gravitational constant  $g$ . Different forms from these variables are grouped and presented as  $X$  and  $Y$  variables in Shields' diagram, where  $X$  has been denoted as  $u_* d / \nu$  and known as particle shear Reynolds number and  $Y$  is  $\tau_{co} / (\gamma_s - \gamma) d$  and known as non-dimensional shear stress. This approach needs an iterative process for determining the incipient motion

Gopu Sreenivasulu is with the Indian Institute of Science, Bangalore. (email: gsrim@civil.iisc.ernet.in).

Bimlesh Kumar is with the Indian Institute of Science, Bangalore. (Corresponding author, phone: 0919886357650, fax: 0918023600404 e-mail: bimk@civil.iisc.ernet.in).

Prof. Achanta Ramakrishna Rao is with the Indian Institute of Science, Bangalore. (e-mail: ark@civil.iisc.ernet.in).

values. Although this approach is used universally, many researchers [2-8] have pointed several limitations of using this method.

The existing methods to design incipient motion in alluvial channels knowingly or unknowingly assume the Manning's roughness coefficient for velocity determination, and this implies of assuming the velocity instead calculating it. This also leads to the erroneous designs of alluvial channels. The mechanism of incipient motion in reality is so complex that it is difficult to model in either a traditional or a conventional manner and the challenge to discover a superior solution continues.

Artificial intelligence modeling systems, where functional, performance, and reliability requirements demand the tight integration of physical processes and information processing, are among the most significant technological developments of the past 20 years [9-10]. This has opened up new opportunities for modeling processes about which either the level of available knowledge is too limited to put the relevant information in a mathematical framework or too little data is available for calibrating an appropriate model. Artificial intelligence modeling has been used in a wide variety of applications, including calibrating water distribution system [11-12], flood management [13], modeling of chemical reactors [14], modeling of aircraft operation [15] and complex ground water modeling [16]. Neural network techniques have been used to study several hydrologic and hydraulic phenomena including water quality, stream flows, rainfall, runoff, sediment transport, and to infill missing data [17]. Caamaño et. al. [18] has used metamodeling technique to derive the bed load sediment transport formula

This paper attempts the application of the neural network technique into the sediment transport problem. The objectives of this study are to develop an RBF neural network model for simulating and predicting incipient motion of alluvial channel and to demonstrate the practical capability and usefulness of this technique.

## II. LIMITATIONS OF MANNING'S COEFFICIENT

Alluvial channels may exhibit significantly differing resistance to flow considering the range of flow conditions and the variety of rivers operating under varying geomorphic conditions and subjected to changes due to developing water resources programs. In order to ascertain responses of alluvial systems, the most important variable is velocity and the

Manning's equation is utilized to determine velocity, if it is not measured. The hydraulic radius and slope of energy gradient are precisely defined but may not always be precisely determined. However, error in determining  $R$  and  $S_f$  can be minimized by careful field measurements and adequate knowledge of river response to varying flows. Resistance to flow can vary significantly with type of alluvial channel, regime of flow, gradient, and geometry of channel, flow, and form of bed roughness, grain roughness, width/depth ratios, bank alignment and vegetation. The hydraulic radius and slope of energy gradient are precisely defined but may not always be precisely determined. Manning  $n$  values are highly variable over time and distance, and generally are much more difficult to estimate accurately especially in open-channel, alluvial flow cases. Inaccuracies of up to one order of magnitude are not uncommon when estimating  $n$  on the basis of inadequate experience and no field data.

There is no single, specific  $n$  value for a given reach of an alluvial stream that experiences different flows. There are numerous  $n$  values, each dependent upon a number of imposed, interdependent variables.

### III. EXPERIMENTATION

Experiments are conducted in two rectangular smooth walled sand bed channels under steady and fairly uniform flow conditions. One channel is smaller in dimensions of 360 cm long 15 cm wide and 20 cm deep where as the second channel is relatively bigger and its dimensions are respectively 1416 cm, 61.5 cm and 80 cm. The first one has plexi glass walls supported on steel frame with a provision of tilting arrangement where as the second one is made out of masonry, which has a fixed horizontal bed slope with smooth (painted) walls. A sand bed with a uniform thickness of 8 cm in smaller channel and 18 cm in the bigger channel was employed.

Quartz silica sands of 4 sizes i.e.,  $d_{50} = 0.44, 0.65, 1.00, 1.77\text{mm}$  along with a gravel of  $8.00\text{mm}$  were used as bed material in the flumes. All sizes are of fairly uniform material having the gradation coefficient of  $\sigma = 0.5(d_{84}/d_{50} + d_{50}/d_{16})$  is in the range of 1.08 to 1.3. Where,  $d_{16}$ ,  $d_{50}$  and  $d_{84}$  are the sizes pertaining to percent finer at 16, 50 and 84 percent respectively. The bed is made plane without any undulations in every experimental run. After setting a desired bed slope,  $S_o$  (in smaller flume only) and a tailgate position, movement of the bed particles is continuously observed by gradually increasing the discharge,  $Q$ . Incipient motion tests are conducted by following Yalin's [19] method of identifying incipient motion in a test reach in which flow is expected to be free from up-stream and down-stream controls and the flow is fully developed. After reaching the stable conditions, the water surface elevations were measured with an accuracy of  $\pm 0.015$  mm of water head at regular intervals along the channel by using a micro manometer [20] to determine the water surface slope  $S_w$ . Flow depths along the central line of the channel were measured at regular intervals using a point gauge of accuracy of 0.10 mm,

in order to obtain the average flow depth,  $y$  over a test reach. The inlet discharge  $Q$  was measured either volumetrically or with the help of a calibrated V-notch. Thus, the basic variables of  $S_o$ ,  $S_w$ ,  $Q$  and  $y$  are obtained in every experimental run. The physical properties like density and unit weight of fluid and sediment particles as well the fluid viscosity are determined by appropriate methods. An over view of the data obtained from the present experiments is shown in the Table 1.

#### A. Data from other sources and their comparison

In order to substantiate the results, additional data from various other sources is also used along with the present experimental data. Various researchers' data [21-25] has been used. Salient features of the experimental data are given in Table 1. It may be noted that all the data are pertaining to plane sediment beds only; however the criteria followed to observe incipient motion vary from one investigator to other. Hence it may be required to compare and contrast their methods of observations to arrive at incipient motion so as to see any significant variations in the data used in the analysis. Yalin's criterion [19] of incipient motion observations is followed in the present as well as in Yalin and Karahan's experiments [24]. Mantz [22] has followed a method of obtaining incipient motion which is similar to Shields [1] extrapolation of sediment rate curves to zero transport. As an alternative, Mantz stated that a same condition may be subjectively estimated by naturally laying a stable sedimentary bed from slowly depositing solids of a shear flow suspension. Mantz [22] has conducted incipient motion runs by increasing the average velocity of the shear flow, until bed forms are observed during deposition and then slightly reduced below the critical stage, a flat bed of maximum stability will be attained. The critical stress can then be estimated subjectively by observation of incipient transport [22] from such beds. Ashida and Bayazit [21] have arrived at incipient motion by extrapolation of the curve between shear stress and sediment discharge to a vanishing transport. According to Vanoni [25], the motion occurred in bursts or gusts produced by the turbulence near the bed and covered areas that were at least of magnitude larger than the viewing area. It may be noted that in spite of several approaches are being followed to arrive at incipient motion by various investigators, the final outcome appears to be more or less the same as demonstrated in data analysis at a later stage.

Figure 1 shows all the incipient data with Shields' diagram in order to verify its incipient condition including several investigators' data with present runs. Rao and Sreenivasulu [26] have fitted an equation to the Shields' functional diagram which fits the incipient motion data reasonably well. Smooth wall correction procedures are not applied in the runs shown in Figure 1 in computing the critical shear stress because of the reason that maximum bed shear stress, which acts along the central region of the channel, can be computed by  $\gamma S_f$  and it is generally valid for the aspect ratios  $B/y \geq 4$  [27]. So also the observations on the incipient motion are made in the same region hence critical shear stress,  $\tau_{co}$  is taken as equal to  $\gamma S_f$  (without wall correction) for  $B/y \geq 4$ . Along with this

condition on aspect ratio, the data used in the analysis is restricted to another condition of relative roughness height  $y/d \geq 3$ , as it is generally difficult to make accurate measurements for relative roughness heights,  $y/d$  less than 3. These two constraints,  $B/y \geq 4$  and  $y/d \geq 3$ , are self-imposed for better understanding of the concepts rather than entering into misjudgments due to unavoidable experimental errors that are likely to creep into the analysis and understanding the concept.

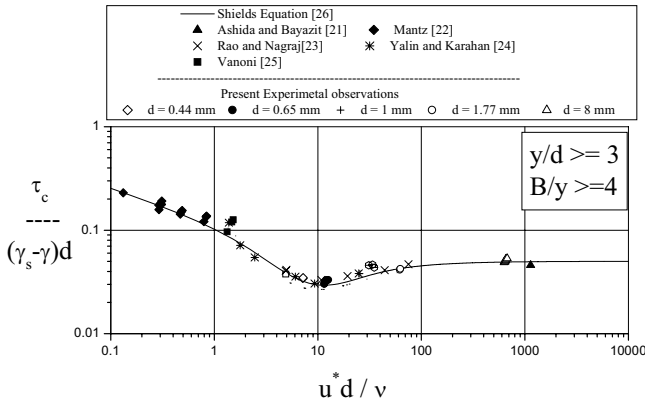


Fig. 1 Shields' Diagram

#### IV. RADIAL BASIS FUNCTION (RBF) MODELING

The Radial Basis Function (RBF) model can be viewed as a realization of a sequence of two mappings. The first is a nonlinear mapping of the input data via the basis functions and the second is a linear mapping of the basis function outputs via the weights to generate the model output. This feature of having both nonlinearity and linearity in the model, which can be treated separately, makes this a very versatile modeling technique [28].

The objective here is to construct a RBF metamodel that approximates an unknown input-output mapping on the basis of given simulation data. The goal, however, is not to provide an exact fit to the data but to develop a metamodel that captures the underlying relationship so that it can be used to predict the output at some future observation of the input. The network consists of three layers: an input layer, a hidden layer and an output layer. The output of the RBF in Figure 2 is calculated according to [28]:

$$\eta(x, w) = \sum_{i=1}^j w_i \phi_j (\|x - \mu_j\|) \quad (1)$$

where  $x$  is input vector matrix,  $\phi$  is a basis function,  $\|\cdot\|$  denotes the Euclidean norm,  $w_i$  are the weights in the output layer,  $j$  is the number of neurons (and centers) in the hidden layer and  $\mu$  is the RBF centers in the input vector space. The first layer (input layer) distributes input vectors to each of the receptive field units in the second layer (hidden layer) without any multiplicative factors. The hidden layer has  $m$  receptive field units (or hidden units), each of which represents a nonlinear transfer function called a basis function. The hidden units play a role in simultaneously receiving the input vector

and nonlinearly transforming the input vector into a  $j$ -dimensional vector. The outputs from the  $j$ -hidden units are then linearly combined with weights to produce the network output at the output layer. There are several common types of functions used, for example, the Gaussian, the multiquadric, the inverse multiquadric and the Cauchy. Present work uses the multiquadric function, which is given as:

$$\phi = \frac{\sqrt{\sigma^2 + (x - \mu)^2}}{\sigma} \quad (2)$$

where parameter  $\sigma$  controls the "width" of the RBF and is commonly referred to as the spread parameter [29]. The RBF model is completely defined by the parameters  $(\sigma, \mu, w)$ . Therefore the RBF design problem is that of determining its  $3j$  parameters, namely,  $j$  centers,  $j$  widths and  $j$  weights. It is quite common in many applications to use a global width. Then the number of parameters to be determined reduces to  $(2j+1)$ . Each of these can have significant impact on the quality of the resulting fit, and good values for each of them need to be determined. The crucial problem is how to select centres appropriately [30]. According to Bian [31], Statistical F test is used to choose the number of centres, and K mean method is used for locating the centres. The basis of K mean method is the criterion for the sum of errors squares. This algorithm also starts from zero centers, and selects centers in a forward selection procedure. The algorithm finds (among the data points not yet selected) the data point with the largest residual, and chooses that data point as the next center. This process is repeated until the optimal number of centers is reached. For deciding the width "TrialWidths" algorithm of Matlab® 7 [32] has been used. This routine tests several width values by trying different widths. A set of trial widths equally spaced between specified initial upper and lower bounds are selected. The width with the lowest value of generalized cross-validation is selected.

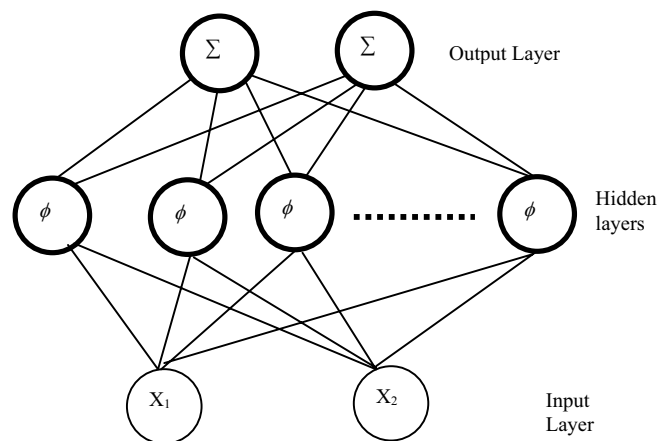


Fig. 2 Structure of a RBF network

Entire modelling work has been done by using MATLAB® 7 [32]. The total numbers of data points at incipient condition are 53. It contains the literature data and

the present experimental data. The basic parameters which define the incipient condition are  $u$ ,  $d$ ,  $y$  and  $S_f$ . Input patterns are  $d$  and  $S_f$  and the output parameters of the model are  $y$  and  $u$ . The main parameter in order to get a good fit with an RBF is the maximum number of centers. To get a better fit different combination of centers, RBF functions and regularisation parameter have been tried.

The best fit model is a radial basis function network using a multiquadric kernel with 13 centers and a global width of 1.8878. The model output and experimental point have been plotted in Figure 3a and 3b. The  $R^2$ , also called multiple correlation or the coefficient of multiple determination, is the percent of the variance in the dependent explained uniquely or jointly by the independents.  $R^2$  can also be interpreted as the proportionate reduction in error in estimating the dependent when knowing the independents. That is,  $R^2$  reflects the number of errors made when using the regression model to guess the value of the dependent, in ratio to the total errors made when using only the dependent's mean as the basis for estimating all cases. Figures 4 shows how well the present model predicts over the design region. Low values of prediction error means that good predictions are obtained at that point.

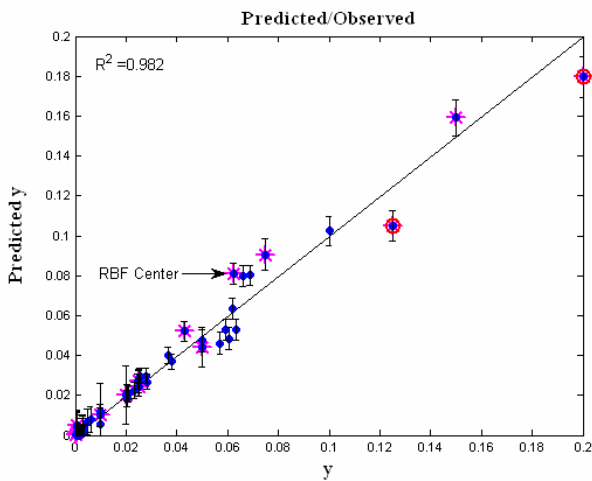


Fig. 3a Modelling result for  $y$

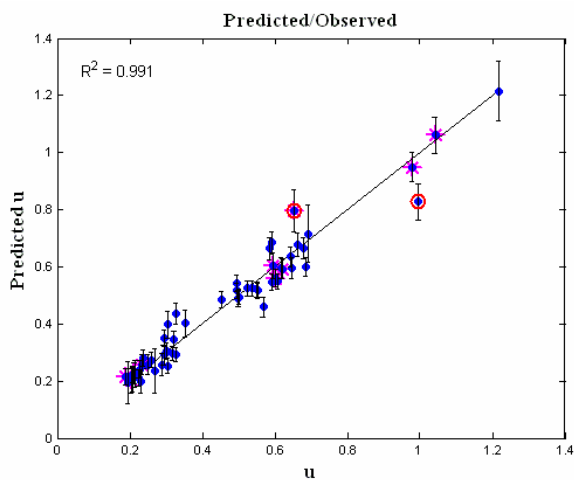


Fig. 3b Modelling result for  $u$

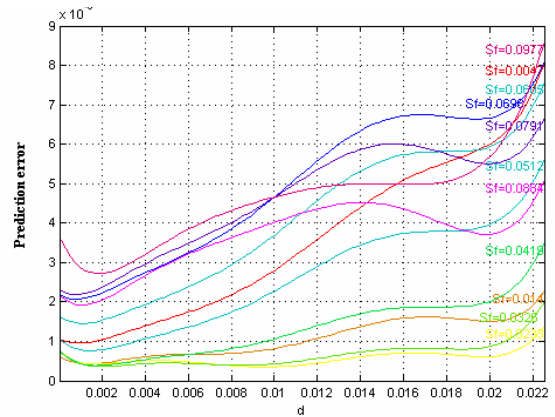


Fig. 4 Prediction error of the model

*A. Design Curves*

There are four basic design variables, namely, particle size  $d$ , flow depth  $y$ , water discharge  $Q$ , and friction/energy slope  $S_f$ . Out of these four variables at least two of them are to be known to solve the remaining two variables. Based on the RBF model, for different values of  $d$  and  $S_f$ , design curves have been generated to predict the values of  $u$  and  $y$ . Subjectivity of these design curves (Figure 5a and 5b) lie in the experimental range covered in the present paper.

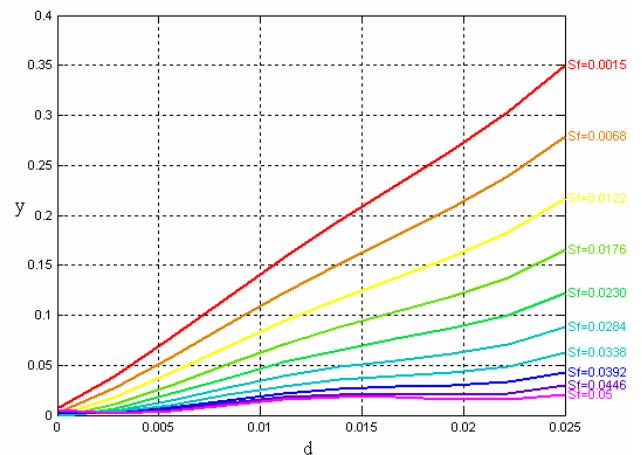


Fig. 5a Design curve for  $y$

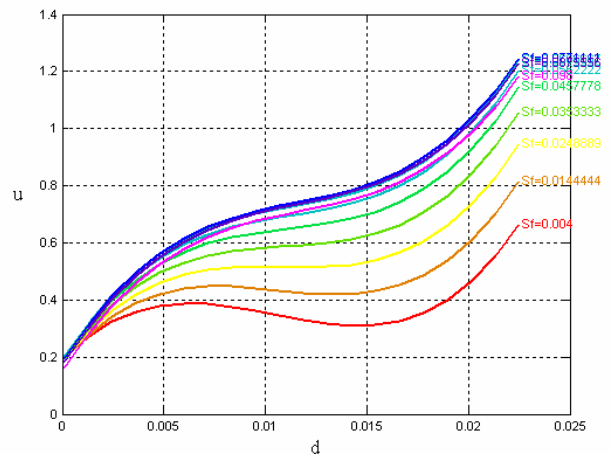


Fig. 5b Design curve for  $u$

## V. CONCLUSION

Traditional parametric design analysis is inadequate for the analysis of large-scale engineering systems because of its computational inefficiency; therefore, a departure from the traditional parametric design approach is required. Approximation techniques may be applied to build computationally inexpensive surrogate models for large-scale systems to replace expensive-to-run computer analysis codes or to develop a model. Although there are several techniques, in this work RBF approach is considered for designing the incipient motion phenomena. The fitting capability of methods is exciting; at the present time it is based on a small set of exemplars. Thus, this approach gives an approximation route of designing the system and at the same time Manning's equation can be avoided while designing the incipient motion in alluvial channels.

## REFERENCES

- [1] Shileds, "Anwendung der Ähnlichkeitsmechanik und Turbulenzforschung auf Geschiebebewegung. Mitteilungen der preuss. Versuchsamt. f. asserbau u. schiffbau, Heft 26, Berlin, 1936.
- [2] J. Buffington and D. Montgomery, "A systematic analysis of eight decades of incipient motion studies, with special reference to gravel bed rivers," *Water Resour. Res.*, 33 (8), 1993–2029, 1997.
- [3] Kumar, "Finding Discharge at Incipient Motion in an Alluvial Channels," ME Thesis, Department of Civil Engg. IISc, Bangalore, 2003.
- [4] J.W. Lavelle and H.O. Mofjeld, "Do critical Stresses for Incipient Motion and Erosion Really Exist?," *Journal of Hydraulic Engg.*, ASCE, 113, 370-385, 1987.
- [5] N.A. Marsh, Andrew W. Western and Rodger B. Grayson, "Comparison of Methods for Predicting Incipient Motion for Sand Bends," *J. Hydraulic Engg. ASCE*, 616-621, 2004.
- [6] D. Taylor and V.A. Vanoni, 1972. "Temperature effects in low-transport flat bed flow," *J. Hydr. Div. ASCE*, 98 (8), 1427-1445, 1972.
- [7] T. Yang, "Unit stream power and sediment transport," *J. Hydr. Div., ASCE*, 98(10), 1805–1826, 1972.
- [8] C. T. Yang, "Incipient motion and Sediment Transport," *J. Hydr. Div., ASCE*, 99(10), 1679-1704, 1973.
- [9] J. P. C. Kleijnen, "Statistical Tools for Simulation Practitioners," New York: Marcel Dekker, 1987.
- [10] J. Sztipanovits, "Engineering of Computer-Based Systems: An Emerging Discipline," Proceedings of the IEEE ECBSJ98 Conference, 1998.
- [11] S. Lingireddy and L. E. Ormsbee, "Neural networks in optimal calibration of water distribution systems," Artificial neural networks for civil engineers: Advanced features and applications, I. Flood and N. Kartam, eds., ASCE, Reston, Va., 53–76, 1998.
- [12] L. Ma, X. Kunlun and L. Suiqing, "Using Radial Basis Function Neural Networks to Calibrate Water Quality Model," *International Journal of Intelligent Systems and Technologies*, 3, 2, 90-98, 2008.
- [13] M. Aqil, I. Kita, A. Yano and N. Soichi, "Decision Support System for Flood Crisis Management using Artificial Neural Network," *International Journal of Intelligent Systems and Technologies*, 1, 1, 70-77, 2006.
- [14] J. R. Kalagnanam and U. M. Diwekar, "An efficient sampling technique for off-line quality control," *Technometrics* 39 (3), 308–319, 1997.
- [15] M. Meckesheimer, A.J. Booker, R.R. Barton and T.W. Simpson, "Computationally inexpensive metamodel assessment strategies," *AIAA J.*, 40(10): 2053–2060, 2002.
- [16] M. Johnson and L. L. Rogers, "Accuracy of neural network approximators in simulation-optimization," *J. Water Resour. Plan. Manage.* 126(2), 48–56, 2000.
- [17] R. S. Govindaraju, "Artificial Neural Networks in Hydrology," Kluwer Academic Publishers, 2000.
- [18] D. Caamaño, P. Goodwin and M. Manic, "Derivation of a bed load sediment transport formula using artificial neural networks," 7th international conference on hydro informatics, Nice, France, 2006
- [19] S. M. Yalin, "Mechanics of Sediment Transport," Pergamon: Tarrytown, NY., 1976.
- [20] R. K. Rao, "A Digital Micro manometer for Very Low Pressure Measurement," *Journal of the Instrument Society of India*, 35, 1, 54-64, 2005.
- [21] K. Ashida and M. Bayazit, "Initiation of motion and roughness of flows in steep channels," 15<sup>th</sup> Congress, IAHR Conference, Istanbul, 1973.
- [22] P. A. Mantz, "Incipient transport of fine grains and flakes by fluids – Extended Shields' diagram", *J. Hydr. Div., ASCE*, 103(6), 601-614, 1977.
- [23] R. K. Rao and N. Sitaram, "Stability and Mobility of Sand-Bed Channels Affected by Seepage," *J. Irri and Drainage, ASCE*, 125 (16), 370-379, 1999.
- [24] S. M. Yalin and E. Karahan, "Inception of Sediment Transport," *J. Hydr. Div., ASCE*, 105 (11), 1979.
- [25] V. A. Vanoni, "Measurement of Critical Shear Stress for Entraining Fine Sediments in a Boundary Layer," Report No. KH-R-7, California Institute of Technology, 1964.
- [26] A.R.K. Rao and G. Sreenivasulu, "Design of Plane Sediment Bed Channels at Critical Condition," *ISH Journal of Hydraulic Engineering*, 12, 94-117, 2006.
- [27] V. Ramana Prasad, "Velocity, Shear and Friction factor studies in rough rectangular open channels for super critical flow," Ph.D. thesis, Indian Institute of Science, Bangalore, 1991.
- [28] S. Haykin, "Neural networks: a comprehensive foundation," Macmillan, New York, 1994.
- [29] F. M. Ham and I. Kostanic, "Principles of Neurocomputing for Science and Engineering," McGraw-Hill India, 2001.
- [30] Feng and Y. Liu, "Status quo and Problems in neural networks control," *Control theory and applications (China)* 11(1), 103-106, 1994.
- [31] Z. Bian, "Pattern recognition," Tsinghua University Press: Beijing, China, 1988.
- [32] MATLAB® Version 7 The mathworks.com

TABLE I  
 EXPERIMENTAL OBSERVATIONS

Source	$d_{50}$ mm	$10^2 y$ m	$10^4 Q$ m <sup>3</sup> /s	$10^4 S_f$	B m
Present Experiments	0.44	2.07 – 3.18	6.10 – 9.90	7.89 – 13.17	0.1575
	0.65	3.00 – 5.89	42.75 – 85.43	5.53 – 11.81	0.6150
	1.00	3.12 – 3.84	13.13 – 14.42	12.78 – 20.24	0.1575
	1.77	1.94 – 3.35	8.51 – 17.54	36.81 – 62.46	-do-
	8.00	2.59 – 3.41	22.60 – 32.36	205.5 – 254.3	-do-
Ashida and Bayazit [21]	6.40	2.40	24.00	250.00	0.20
	12.00	3.65	50.00	250.00	-do-
Mantz [22]	0.015	6.01	26.30	0.92	0.30
	0.030	2.27 – 5.86	9.93 – 32.30	1.52 – 3.46	-do-
	0.045	2.43 – 5.96	11.90 – 36.10	1.80 – 4.06	-do-
	0.066	2.46 – 6.07	13.50 – 42.80	2.42 – 5.14	-do-
Rao and Nagaraj [23]	0.32	1.90 – 2.68	6.68 – 8.00	8.10 – 11.17	0.1575
	0.80	2.70	13.00	17.52	-do-
	1.30	3.15	15.75	28.33	-do-
Yalin and Karahan [24]	0.10	0.65	2.25	30.00	0.15
	0.14	0.55	1.69	30.00	-do-
	0.19	0.57	1.78	30.00	-do-
	0.40	0.47	1.50	50.00	-do-
	0.56	0.47	1.52	60.00	-do-
	1.00	0.63	2.72	100.00	-do-
Vanoni [25]	0.102	9.327-11.92	90.61-116.10	-	0.39